



H. M. Azamathulla
Senior Lecturer, River Engineering and Urban Drainage Research Centre (REDAC), Universiti Sains Malaysia, Penang, Malaysia



A. A. Ghani
Deputy Director, River Engineering and Urban Drainage Research Centre (REDAC), Universiti Sains Malaysia, Penang, Malaysia



N. Azazi Zakaria
Director, River Engineering and Urban Drainage Research Centre (REDAC), Universiti Sains Malaysia, Penang, Malaysia

ANFIS-based approach to predicting scour location of spillway

H. M. Azamathulla ME, PhD, A. A. Ghani MSc, PhD and N. Azazi Zakaria MSc, PhD

A spillway with a trajectory bucket as an energy dissipator satisfies the requirements of both safety and economy. Many researchers have developed empirical formulae to predict scour location considering different hydraulic parameters and bucket configurations. An attempt has been made in this paper to estimate the location of maximum scour using parameters such as q , H_1 , R , d_{50} , d_w and the lip angle of the bucket using an adaptive neuro fuzzy inference system (ANFIS). Extensive experimental results were collected and analysed in order to investigate the effect of different parameters on throw distance and scour location downstream of a trajectory bucket spillway. It was found that the scour parameter is a function of the fall Froude number, ratio of head to tailwater depth, ratio of radius of trajectory bucket to head, ratio of sediment mean size to head and lip angle of the bucket. The functional relationship is expressed in dimensionless form. This paper also presents an alternative to the regression in the form of neural fuzzy modelling. The results of this modelling were compared with the regression equation and it was found that the ANFIS results are highly satisfactory. The results of this study can be used to predict the location of maximum scour downstream of the trajectory bucket spillway.

1. INTRODUCTION

The use of a trajectory bucket spillway with a plunge pool can be a safe and economical means of energy dissipation of dams. The trajectory bucket energy dissipator is able to throw the jet at a relatively safe distance from the bucket lip. It has some economic advantages over other energy dissipators. When geologic and topographic conditions permit, a trajectory bucket (also called flip bucket and ski-jump bucket) type of energy dissipator is generally the most economical at sites with geological hard strata. The plunge pool develops as a result of self-excitation of the bed from jet energy at the point of impact. For sites in which the bed materials are not strong enough to tolerate the high energy of the jet, the construction of a pre-excavated plunge pool is necessary as it dissipates energy by throwing the jet of water at a sufficient distance away from the spillway bucket. The scour hole is usually formed downstream of the point of impingement of the ski-jump jet. The retrogression of this scour hole may cause danger to the stability of the structure by causing a structural failure or by increased seepage. The loss of stability of the

downstream river bed and side slopes and the formation of a mound of eroded material that raises the tailwater level are other undesirable effects of such a dissipator.

It is important to ensure that the scour will not progress upstream to the extent that the safety of the structure might be in danger. High-velocity flow leaving the trajectory bucket will form a large amount of spray as it is dispersed into the air. The ski-jump jet also spreads laterally in the downstream direction abrading the side banks. Therefore, suitable protection for the excavated banks is necessary. Transverse slopes on both flanks of the plunge pool may be chosen, based on geological conditions prevailing at the site. It is also necessary to protect the toe of the dam from undermining owing to the flow cascading over the lip of the bucket. This can be done by providing a concrete apron downstream of the flip bucket. Buckets may be high or low, depending upon their location with respect to the riverbed. Scour locations are directly affected by tailwater level and currents downstream, which alter the path of the jet entering the water. As a result it is likely that scour location is shifted further downstream than the actual jet trajectory indicates.

Over a period of several decades many investigators have given empirical formulae based on laboratory as well as prototype observations in order to predict the scour location downstream of the flip bucket spillway. Those formulae are very convenient to use but have a major drawback in that they involve idealisation, approximation and averaging of widely varying prototype conditions. As a result, the predicted scour locations can be considerably different than their actual values. Apart from the complexity of the phenomenon, this could also be attributable to the limitation of the analytical tools used by most of the earlier investigators, namely statistical regression.

The use of a soft computing tool such as artificial neural networks (ANN) in place of regression for the problem under consideration met with success as shown in Azamathulla *et al.*¹ This inspired the present work in which the scour problem is tackled with the help of another soft computing tool – adaptive neuro fuzzy inference system (ANFIS) – which is extremely flexible in data mining. In the current study the ANFIS is employed to predict the location of maximum scour downstream of the trajectory bucket spillway involved. The scour depth location would be useful information for designing the plunge pool.

1.1. Neural fuzzy modelling

The ANFIS, first introduced by Jang,² is a universal approximator and, as such, is capable of approximating any real continuous function on a compact set to any degree of accuracy.³ Thus, in parameter estimation, where the given data are such that the system associates measurable system variables with an internal system parameter, a functional mapping may be constructed by ANFIS that approximates the process of estimation of the internal system parameter.

The integration of the techniques of fuzzy systems and neural networks (NNs) suggests the novel idea of transforming the burden of designing fuzzy systems to the training and learning of the neural networks. The NNs provide ‘connectionist’ structures (fault tolerance and distributed properties) and learning abilities to the fuzzy systems whereas the fuzzy systems offer NNs a structure framework with high-level IF–THEN rule thinking and reasoning. The neural fuzzy system – one form of integration of fuzzy systems and NNs – is a fuzzy system that uses a learning algorithm derived from or inspired by NN theory to determine its parameters (fuzzy memberships and fuzzy rules) by processing data. In other words, neural fuzzy systems aim at providing fuzzy systems with the automatic tuning methods of NNs without altering their functionality. In a neural fuzzy system, the NN helps the fuzzy system to elicit membership functions, map fuzzy sets to fuzzy rules and implement defuzzification.

The process of constructing a neural fuzzy system is called ‘neural fuzzy modelling’ or ‘neuro-fuzzy modelling’. It consists of the design of a fuzzy system and an NN that equips the fuzzy system with learning capability. Generally, the commonly used fuzzy systems are rule-based fuzzy systems, and the NNs used are mainly multilayer feed-forward networks with the back-propagation learning algorithm. Several paradigms of neural fuzzy modelling are available in the literature such as fuzzy inference networks,⁴ fuzzy aggregation networks,⁵ neural network-driven fuzzy reasoning,⁶ fuzzy modelling networks,⁷ ANFIS² and fuzzy associative memory systems.⁸ Commercial computing software, such as Matlab³ and Fuzzy-tech, provide some encoded algorithms for developing ANFIS and fuzzy associative memory systems respectively. ANFIS is adopted in this study to serve as a basis of the neural fuzzy model for estimation of scour location downstream of a flip bucket.

2. LITERATURE REVIEW

Several investigators such as Maitre and Obolensky,⁹ Horeni,¹⁰ Elevatorski,¹¹ Kawakami,¹² Elsawy and McKeogh,¹³ Taraimovich,¹⁴ Kobus *et al.*,¹⁵ Sen,¹⁶ Locher and Hsu,¹⁷ Bormann and Julien,¹⁸ Breusers and Raudkivi,¹⁹ Zhenghu,²⁰ Amanian and Gilberto,²¹ Tao,²² Mason,²³ Rae and Diana,²⁴ Hoffmans and Verheij,²⁵ Hoffmans,²⁶ Ghodsian *et al.*,²⁷ Roman and Hager²⁸ and Stefano and Hager²⁹ have studied the free-flow jet trajectory and have developed relationships for maximum jet-trajectory length owing to free jet in the form of dimensional equations. Many of these studies were directed towards predicting maximum trajectory length and these formulae did not indicate the likely maximum scour location. Less attention was paid to other scour hole parameters such as the length of the scour, the width of the scour and the distance of maximum scour point from the bucket lip. Data on trajectory lengths have generally been obtained from hydraulic models.

Probably the most important consideration in the design of the trajectory bucket is to determine how far the jet will be deflected downstream. Theoretically, if friction is neglected, regardless of air and the disruption of the jet, the following equation can be used to compute the horizontal component of the jet trajectory

$$1 \quad \chi = \frac{v_o^2 \sin 2\phi}{g}$$

where v is velocity, ϕ is the bucket lip angle with the horizontal and g is acceleration due to gravity.

Equation 1 can be transformed into dimensionless forms by dividing each side of the equation by H , which is the vertical distance between the maximum pool and the river bed¹¹

$$2 \quad \frac{\chi}{H} = 2 \frac{h}{H} \sin 2\phi$$

Measurements made by Maitre and Obolensky at the St Etienne Cantales and Chastang Dams in France for flows which were less than one-half the maximum discharge showed that approximately 19–20% of the total energy is dissipated by the interaction of the jet during its flight. They thus suggested that

$$3 \quad \frac{\chi}{H} = 1.9 \frac{h}{H} \sin 2\phi$$

Obviously the maximum value of $\sin 2\phi$ in Equation 3 is unity. Consequently the maximum jet-trajectory length will occur at a 45° lip angle of the bucket. Maitre and Obolensky⁹ also presented theoretical curves for the relationship χ/H and h/H for bucket lip angles ranging from 10° and 45° based on experiments which Panasenkov³⁰ also used in plots. It was concluded that the data agreed very well with the theoretical curves. They also found that the trajectory lengths observed in the model tests for exit angles ranging from 25°45’ and 45°45’ were slightly greater than those yielded by Equation 3.

In the design of trajectory buckets, the designer may also wish to determine the vertical component, or height, of the jet trajectory. If air resistance and the disruption of the jet are neglected, the following equation can be used to compute jet-trajectory height

$$4 \quad y = \frac{v_o^2 \sin^2 \phi}{2g}$$

As $v_o^2/2g = h$, Equation 4 becomes

$$5 \quad \frac{y}{h} = \sin^2 \phi$$

Neither Equation 3 nor Equation 5 accounts for the changes in the bucket radii which affects both the length and the height of the jet trajectory. The present paper describes the importance of the bucket radii (R) and discharge intensity (q) in the derivation of both the length and the height of the jet trajectory.

Horeni¹⁰ derived a trajectory length equation by using hydraulic model data. He found that

$$6 \quad L_0 = 5.88q^{0.319}$$

where L_0 is length from the overfall edge measured along the jet axis in cm and q is discharge intensity in cm^2/s .

Elsawy and McKeogh,¹³ in their model study, determined the disintegrated length in the form of formula for trajectory length as follows

$$7 \quad L_0 = 10.50q^{0.33}$$

The United States Bureau of Reclamation Service (USBR) equation for free jet trajectory length (X_h) gives

$$8 \quad X_h = h_c \sin 2\theta + 2 \cos \theta [h_c (h_c \sin^2 \theta + Y_1)]^{1/2}$$

where h_c is the velocity head at the bucket lip in metres, Y_1 is the vertical distance below the bucket lip to the impact area in feet and θ is the angle between the horizontal and the floor at the beginning of the trajectory, in degrees.

Kawakami¹² obtained the results of some field investigations of jet trajectories for ski-jump spillway and introduced a coefficient related to air resistance, k , for the following trajectory equations

$$9a \quad y = \frac{1}{gk^2} \ln (\cos \gamma + \tan \alpha \sin \gamma)$$

$$9b \quad L_1 = \frac{1}{gk^2} \ln (1 + 2k\alpha V_0 \cos \theta)$$

where

$$9c \quad \alpha = \tan^{-1} (kV_0 \sin \theta) \quad (\text{rad})$$

$$9d \quad \gamma = \frac{\exp(gk^2 x) - 1}{kV_0 \cos \theta} \quad (\text{rad})$$

x and y are Cartesian coordinates, V_0 is in m/s and θ is as defined in Figure 1. L_1 is the throw distance which corresponds to

$$L_0 = \frac{V_0^2}{g} \sin 2\theta$$

Kawakami developed an empirical relationship between V_0 and k . He used data from field tests and developed the relationship of L_1/L_0 as a function of V_0 . He also concluded that the effect of air resistance is small whenever V_0 is less than about 20 m/s but when velocity increases to 40 m/s the throw distance could

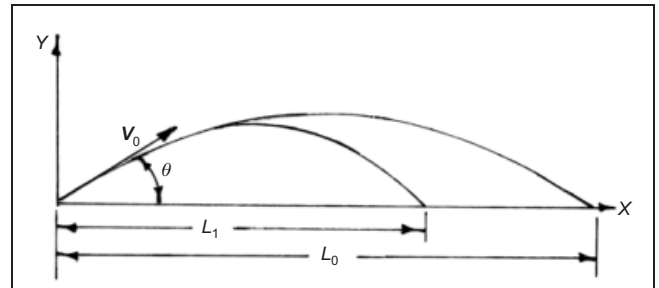


Figure 1. Jet trajectory with and without air resistance

be reduced by as much as 30% from the L_0 . Kawakami's results provide a basis for estimating the effects of air resistance.

The Bureau of Indian Standards³¹ (BIS 7365-1985) relationship for the throw distance of the trajectory buckets is as follows

$$10 \quad \frac{x}{H_v} = \sin 2\phi + 2 \cos \phi \left(\sin^2 \phi + \frac{y}{H_v} \right)^{1/2}$$

where x is the horizontal throw distance from the bucket lip to the centre point of impact with tailwater in metres, y is the difference between the lip level and the tailwater level (the sign is taken as positive for tailwater below the lip level and negative for tailwater level above the lip level in metres); H_v is the velocity head of the jet at the bucket lip in metres; and ϕ is the bucket lip angle with the horizontal in degrees.

BIS also specified that for the conditions when y is negative, model studies may be carried out to confirm the values of horizontal throw distance (x) and vertical distance (a).

$$11 \quad a = \frac{v_a^2 \sin^2 \phi}{2g}$$

where a is vertical distance from lip level to the highest point of the centre of jet in metres, v_a is actual velocity of flow entering the bucket in m/s and g is acceleration owing to gravity in m/s^2 .

Taraimovich's formula for maximum scour location from bucket lip is

$$L_{fr} \geq 7 h_{cr}$$

where L_{fr} is the range of take-off of the jet from the ski-jump for its lower design limit and h_{cr} is the critical depth at the bucket lip. He also mentioned the criterion for the stability of the upstream slope of the scoured hole below the arch dams. The relationship indicates L_{fr} is a function of the unit discharge.

Tao's theoretical formula for the length of nappe jetting is

$$12 \quad L = 2\phi^2 s \cos \alpha \left[\sin \alpha + \sqrt{\left(\frac{\sin^2 \alpha + [(h/2) \cos \alpha + s_1]}{\phi^2 s} \right)} \right]$$

where ϕ is the velocity coefficient at the lip, which can be determined by using the empirical formula as given below; s is the drop in elevation between the reservoir water level and the top of the bucket lip (m), s_1 is the drop in the elevation between the lip and the tailwater level (m); h is the water depth above the lip (m), and α is the angle of emergency for the high lip.

13	$\phi = 2 \left(\frac{q}{g^{0.5} L^{1.5}} \right)^{0.21}$
----	--

3. DIMENSIONAL ANALYSIS

Owing to the complexity of the problem and the lack of theoretical explanations for the development of scour below the trajectory bucket spillway, the employment of dimensional analysis is suggested in order to reduce the number of variables and to assist in the experimental design. Scour geometry depends on many variables that characterise the trajectory bucket and the plunge pool, the bed material and the flow. Referring to Figure 2, the distance for maximum scour depth from the spillway bucket lip (l_s) can be written as a function of the discharge per metre width or unit discharge of spillway (q), total head (H_1), radius of the bucket (R), lip angle of the bucket (ϕ), tailwater depth (d_w), mean sediment size (d_{50}) and the acceleration due to gravity (g)

14	$l_s = f(q, H_1, R, \phi, d_w, d_{50}, g)$
----	--

Using the Buckingham π theorem, this expression can be reduced to

15	$\frac{l_s}{H_1} = f \left(\frac{q}{\sqrt{gH_1^3}}, \frac{d_w}{H_1}, \frac{R}{H_1}, \frac{d_{50}}{H_1}, \phi \right)$
----	--

The above functional relationships are the focus of the present study.

4. EXPERIMENTAL DATA COLLECTED

Extensive experimental data were obtained from hydraulic model studies conducted at the Central Water and Power Research Station (CWPRS), Pune, India. In addition, information available in the literature was also used to arrive at the expressions for predicting scour hole parameters. Table 1 shows the range of experimental results collected from these sources. The scour measurements were taken after the equilibrium state was achieved.

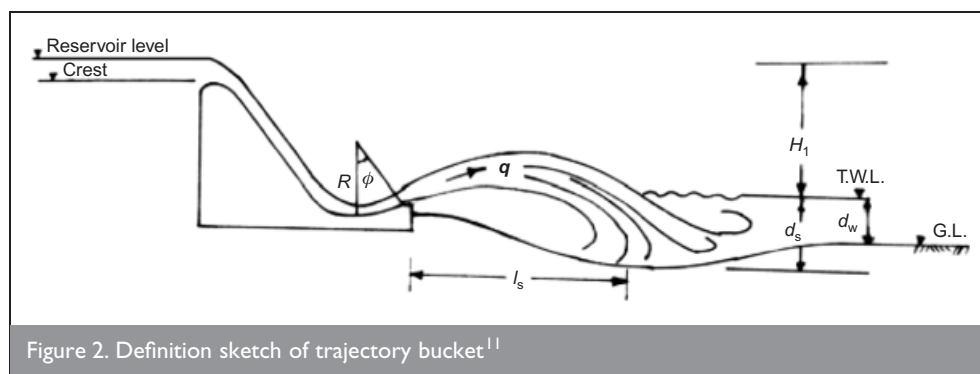


Figure 2. Definition sketch of trajectory bucket¹¹

The dataset used in this study consists of the original experimental data available at CWPRS, India, in addition to available published data. Past measurements of scour parameters made during numerous laboratory investigations carried out at the CWPRS in India were first compiled for potential use in the current study. These hydraulic model studies were conducted on various sectional as well as comprehensive models. The sectional models were scaled to the range of 1:40 to 1:60 whereas comprehensive models had their scales varied from 1:50 to 1:100.

A review of these observations revealed that additional measurements were necessary in order to make them more comprehensive, especially with respect to the pattern of scour including the width and the distance of maximum scour depth from the spillway bucket lip (length). New hydraulic model studies were therefore conducted on three different bucket designs. The three hydraulic models simulated the dams across the Subarnarekha, Ranganadi and Parbati Rivers in India. Dr Masoud Ghodsian of Tarbiat Modarres University, Tehran, Iran also kindly provided additional scour data results from his previous work.²⁷

5. ANALYSIS

Eighty per cent of the observations were used to arrive at the expressions for predicting the equilibrium scour hole parameters according to the functional relationship given by Equation 16. By using the non-linear regression analyses, the following equations were obtained for estimating the distance of maximum scour location

16	$\begin{aligned} \frac{l_s}{H_1} = & 9.85 \left(\frac{q}{\sqrt{gH_1^3}} \right)^{0.42038} \left(\frac{d_w}{H_1} \right)^{0.007} \\ & \times \left(\frac{R}{H_1} \right)^{0.0432} \left(\frac{d_{50}}{H_1} \right)^{0.03702} (\phi)^{0.346} \end{aligned}$
----	---

The constants in the above equation were worked out on the basis of the least square fit to 80% of randomly selected values, which contains minimum and maximum values. The use of the Origin software in the windows platform was made for this purpose. The validation of this equation was done with the help of the remaining 20% of the observations which were not involved in the derivation. Figure 3 shows the comparison between the calculated scour location using the above Equation 16 and observed values. The quantitative comparison (Appendix 2), in terms of the values of the correlation coefficient, r , average percentage error, e , average absolute deviation, d , and the mean square error (MSE), is shown in Table 2, which indicates that the r^2 value is as high as 0.964 while e , d and MSE values are as low as 12.84% and 11.35 and 10.89 respectively. This indicates satisfactory estimates of the scour location. It can also be seen from Table 2 that the location of the scour hole is predicted fairly satisfactorily

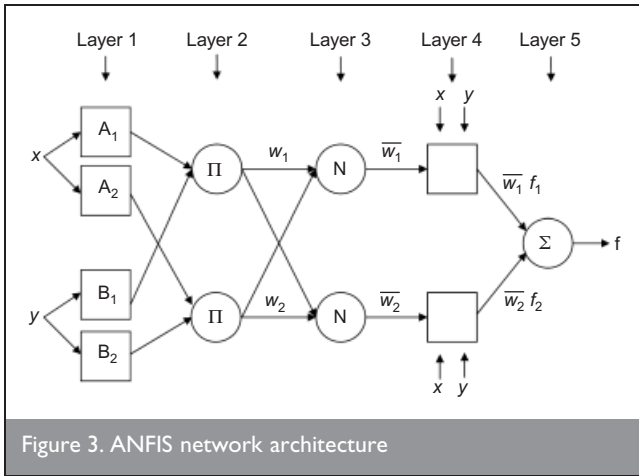


Figure 3. ANFIS network architecture

with 12.84% average error. It is evident that most of the data points fall in the bandwidth of $\pm 10\%$ line. It should also be noted that the data set, which includes 95 data points, covers a wide range of pertinent parameters.

Despite analysing a wide range of model data, the problem of prediction of maximum scour location has remained inconclusive. It is felt that this is partly attributable to the complexity of the phenomenon involved and partly because of the limitation of the analytical tool commonly used by most of the earlier investigators, namely statistical regression. Conventional statistical analysis is now being replaced in many cases by the alternative approach of NNs. Neural networks have advantages over statistical models such as their data-driven nature, model-free form of predictions and tolerance to data errors.

6. THE NETWORKS

An NN represents the interconnection of neurons, each of which basically carries out the task of combining the multiple inputs, determining its strength by comparing the combination with a bias (or alternatively passing it through a non-linear transfer function) and firing out the result in proportion to such a strength as indicated below

17	$O = 1/[1 + e^{-S}]$
----	----------------------

18	$S = (x_1 w_1 + x_2 w_2 + x_3 w_3 + \dots) + \theta$
----	--

where O is output from a neuron; x_1, x_2, \dots are input values; w_1, w_2, \dots represent weights along the linkages connecting any two neurons and indicating strengths of the connections; θ is bias value. Equation 17 indicates a transfer function with a sigmoid nature, which is commonly used, although there are other forms available, such as sinusoidal, Gaussian and hyperbolic tangent. Textbooks^{8,32} give theoretical details of the working of an ANN. The known input-output patterns are first used to train a network; the strengths of interconnections (or weights) and bias values are fixed accordingly. Thereafter, the network becomes ready for application to any unseen real-world example. A supervised type of training involves feeding input-output examples until the network develops its generalisation capability, while an unsupervised training would involve classification of the input into clusters by some rule. In

the supervised training, the network output is compared with the desired or actual one, and the resulting error, or the difference, is processed through a mathematical algorithm. Normally, such algorithms involve an iteration process continuously to change the connection weights and bias until the desired error tolerance is achieved. The traditional training method is standard back-propagation, although numerous training schemes are available to impart better training with the same set of data, as indicated by Londhe and Deo³³ in their harbour tranquility studies.

Most of the previous works that address ANN applications to water resources have included the feed-forward type of architecture, where there are no backward connections, which are trained using the error back-propagation scheme or the FFBP configuration. The ANFIS on the other hand is a hybrid scheme which uses the learning capability of the ANN to derive the fuzzy IF-THEN rules with appropriate membership functions worked out from the training pairs leading finally to the inference.^{34,35} The difference between the common NN and the ANFIS is that while the former captures the underlying dependency in the form of the trained connection weights, the latter does so by establishing the fuzzy language rules. The input in ANFIS (Figure 3) is first converted into fuzzy membership functions, which are combined together. After following an averaging process to obtain the output membership functions, the desired output is finally achieved. The treatment of data non-linearities in this way has been recently found to be useful in fields such as hydrology,³⁶ traffic engineering³⁷ and soil analysis.³⁸ Mathematical expressions involved in the working of the ANFIS are given in Appendix 1.

The following scenarios are considered in building the ANFIS model (Figure 4) with the inputs ($F_0 = q/(gH_1^3)^{1/2}$, d_w/H_1 , R/H_1 , d_{50}/H_1) and ϕ the output (I_s/H_1) shown in the network. After the input and output parameters were determined, genfis2 was employed to generate first-order Sugeno fuzzy system and the ANFIS architectures are similar as they have the same number of inputs and rules. Two membership functions were found sufficient for the estimation of scour location (see Figure 4). Figure 4 depicts the schematic structure of ANFIS model I_s/H_1 . In order to map the causal relationship related to the scour, an input-output scheme was employed, where non-dimensional groupings were utilised.

From the collected data sets used in this study, around 80% of these patterns were used for training (chosen randomly until the best training (calibration) performance was obtained), while remaining patterns (20%) were used for testing, or validating, the ANFIS model. From Table 2 and Figure 5 it is clear that

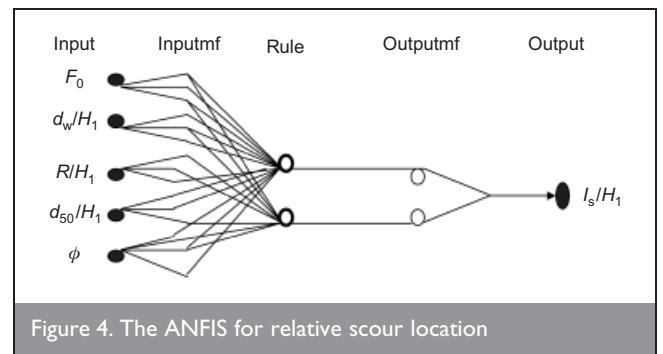


Figure 4. The ANFIS for relative scour location

Sl No.	Discharge intensity, q : (m ³ /s)/m	Total head, H_1 : m	Bucket radius, R : m	Bed material size, d_{50} : m	Lip angle, ϕ : rad	Tail water depth, d_w : m	Location of max. scour lip, l_s : m	Data source
1	0.1703	0.5083	0.400	0.004	0.472	0.1667	1.1116	A
2	0.1792	1.4268	0.406	0.002	0.612	0.2300	1.9512	A
3	0.0842	1.4268	0.609	0.002	0.698	0.1500	2.0202	A
4	0.0634	1.1328	0.406	0.002	0.612	0.0300	0.9807	A
5	0.0266	1.3659	0.610	0.002	0.698	0.1700	0.9756	A
6	0.1616	1.7962	0.254	0.002	0.349	0.2337	1.9055	A
7	0.0709	1.4146	0.610	0.002	0.698	0.1600	1.7378	A
8	0.0204	0.3505	0.180	0.008	0.524	0.0286	0.6970	A
9	0.0374	0.3328	0.140	0.008	0.524	0.0687	0.7200	A
10	0.0093	1.0718	0.406	0.002	0.612	0.2340	0.5742	A
11	0.1239	1.3659	0.406	0.002	0.612	0.1800	1.4634	A
12	0.1446	1.3902	0.406	0.002	0.612	0.2650	1.6463	A
13	0.0399	1.3902	0.610	0.002	0.698	0.1800	1.4329	A
14	0.0471	0.3827	0.140	0.008	0.524	0.0286	0.7500	A
15	0.0204	0.3104	0.180	0.008	0.524	0.0687	0.5000	A
16	0.0204	0.2991	0.140	0.005	0.524	0.1000	0.5300	A
17	0.0186	1.0822	0.406	0.002	0.612	0.2150	0.7165	A
18	0.0285	0.3188	0.140	0.008	0.524	0.0687	0.6300	A
19	0.1616	1.7962	0.254	0.002	0.780	0.2337	2.0709	A
20	0.0471	0.3676	0.140	0.008	0.524	0.0437	0.7000	A
21	0.0089	1.3415	0.610	0.002	0.698	0.1780	0.5183	A
22	0.0725	1.3415	0.406	0.002	0.612	0.0900	0.9146	A
23	0.0250	1.0922	0.406	0.002	0.612	0.2500	0.8781	A
24	0.1616	1.7962	0.254	0.002	0.174	0.2337	1.4482	A
25	0.1626	1.4146	0.406	0.002	0.612	0.2480	1.8902	A
26	0.0870	1.1532	0.406	0.002	0.612	0.0330	1.0163	A
27	0.1616	1.7962	0.254	0.002	0.523	0.2337	2.1439	A
28	0.0204	0.3354	0.100	0.008	0.524	0.0437	0.4950	A
29	0.0398	1.3902	0.610	0.002	0.698	0.1800	1.4329	A
30	0.0285	0.3589	0.250	0.008	0.567	0.0286	0.6500	B
31	0.0435	1.1125	0.300	0.002	0.612	0.2480	0.9502	B
32	0.0374	0.3328	0.250	0.003	0.567	0.0687	0.7000	B
33	0.0374	0.3015	0.250	0.008	0.567	0.1000	0.6700	B
34	0.0374	0.3015	0.250	0.002	0.567	0.1000	0.6500	B
35	0.0471	0.3827	0.250	0.008	0.567	0.0286	0.8200	B
36	0.0285	0.3188	0.250	0.008	0.567	0.0687	0.6400	B
37	0.0204	0.2991	0.250	0.008	0.567	0.1000	0.4550	B
38	0.0285	0.2875	0.300	0.002	0.612	0.1000	0.5500	B
39	0.1532	1.0750	0.560	0.002	0.611	0.1460	1.8400	B
40	0.0511	0.9650	0.560	0.002	0.611	0.1460	1.3400	B
41	0.2042	1.1300	0.560	0.002	0.611	0.1460	2.0400	B
42	0.1021	1.0300	0.560	0.002	0.611	0.1460	1.8000	B
43	0.2042	1.4740	0.560	0.002	0.611	0.1460	2.2400	B
44	0.1532	1.4850	0.560	0.002	0.611	0.1460	2.1440	B
45	0.0511	1.5050	0.560	0.002	0.611	0.1460	1.8400	B
46	0.1021	1.5000	0.560	0.002	0.611	0.1460	2.2400	B
47	0.0285	0.3589	0.180	0.008	0.524	0.0286	0.6500	C
48	0.0374	0.3578	0.140	0.008	0.524	0.0437	0.7100	C
49	0.0471	0.3113	0.140	0.008	0.524	0.1000	0.6000	C
50	0.0285	0.2875	0.180	0.008	0.524	0.1000	0.6300	C
51	0.0374	0.3578	0.200	0.008	0.524	0.0437	0.7250	C
52	0.0471	0.3827	0.180	0.008	0.524	0.0286	0.7800	C
53	0.0471	0.3676	0.180	0.008	0.524	0.0437	0.7750	C
54	0.0204	0.3354	0.100	0.008	0.524	0.0437	0.4950	C
55	0.0285	0.2875	0.200	0.008	0.524	0.1000	0.6200	C
56	0.0285	0.3438	0.180	0.003	0.524	0.0437	0.6500	C
57	0.0471	0.3426	0.180	0.008	0.524	0.0687	0.7800	C
58	0.0374	0.3328	0.180	0.008	0.524	0.0687	0.7000	C
59	0.0374	0.3578	0.180	0.008	0.524	0.0437	0.7100	C
60	0.0471	0.3113	0.100	0.008	0.524	0.1000	0.7000	C
61	0.0204	0.3505	0.200	0.008	0.524	0.0286	0.5250	C
62	0.0471	0.3426	0.100	0.008	0.524	0.0687	0.7200	C
63	0.0374	0.3015	0.140	0.008	0.524	0.1000	0.7000	C
64	0.0285	0.3438	0.200	0.008	0.524	0.0437	0.6500	C
65	0.0285	0.3589	0.140	0.008	0.524	0.0286	0.5800	C
66	0.0204	0.3354	0.200	0.008	0.524	0.0437	0.4700	C
67	0.0204	0.3104	0.100	0.008	0.524	0.0687	0.4500	C
68	0.0204	0.3505	0.140	0.008	0.524	0.0286	0.5000	C
69	0.0285	0.2875	0.140	0.008	0.524	0.1000	0.6000	C

(continued)

Sl No.	Discharge intensity, q : (m ³ /s)/m	Total head, H_1 : m	Bucket radius, R : m	Bed material size, d_{50} : m	Lip angle, ϕ : rad	Tail water depth, d_w : m	Location of max. scour lip, l_s : m	Data source
70	0.0471	0.3827	0.100	0.008	0.524	0.0286	0.8150	C
71	0.0374	0.3729	0.200	0.008	0.524	0.0286	0.7500	C
72	0.0285	0.3589	0.100	0.008	0.524	0.0286	0.6100	C
73	0.0471	0.3426	0.200	0.008	0.524	0.0687	0.7200	C
74	0.0471	0.3676	0.200	0.008	0.524	0.0437	0.7600	C
75	0.0204	0.3304	0.140	0.008	0.524	0.0687	0.5000	C
76	0.0204	0.3354	0.180	0.008	0.524	0.0437	0.6600	C
77	0.0285	0.3438	0.100	0.008	0.524	0.0437	0.6050	C
78	0.0471	0.3426	0.140	0.008	0.524	0.0687	0.6700	C
79	0.0471	0.3113	0.250	0.008	0.524	0.1000	0.6900	C
80	0.0204	0.3505	0.100	0.008	0.524	0.0286	0.4900	C
81	0.0374	0.3328	0.100	0.008	0.524	0.0687	0.6600	C
82	0.0471	0.3676	0.100	0.008	0.524	0.0437	0.7300	C
83	0.0204	0.3104	0.200	0.008	0.524	0.0687	0.5000	C
84	0.0285	0.3438	0.140	0.008	0.524	0.0437	0.6500	C
85	0.0285	0.3188	0.180	0.008	0.524	0.0687	0.6500	C
86	0.0204	0.2791	0.100	0.008	0.524	0.1000	0.5000	C
87	0.0374	0.3729	0.140	0.008	0.524	0.0286	0.7400	C
88	0.0471	0.3113	0.180	0.008	0.524	0.1000	0.7650	C
89	0.0285	0.3188	0.100	0.003	0.524	0.0678	0.5550	C
90	0.0204	0.3354	0.140	0.008	0.524	0.0437	0.4200	C
91	0.0374	0.3015	0.180	0.008	0.524	0.1000	0.6850	C
92	0.0374	0.3578	0.100	0.008	0.524	0.0437	0.7150	C
93	0.0374	0.3729	0.180	0.008	0.524	0.0286	0.7200	C
94	0.0374	0.3729	0.100	0.008	0.524	0.0286	0.7200	C
95	0.0204	0.2791	0.180	0.008	0.524	0.1000	0.5500	C
Min.	0.0089	0.2791	0.100	0.002	0.174	0.0286	0.4200	
Max.	0.2042	1.7962	0.610	0.008	0.780	0.2650	2.2400	

A: Numerous research reports of hydraulic model studies conducted at Central Water and Power Research Station, India. B: New model studies in respect of dams along river, Subernarekha, Ranganadi and Parbati. C: Personal communication from Dr Masoud Ghodsian of Tarbiat Modarres University, Tehran, Iran.

Table 1. The database used

Method	Coefficient of correlation, r	Coefficient of determination, r^2	Average error, AE: %	Mean absolute deviation, d	Mean square error, MSE
Regression (authors' Equation 16)	0.93	0.864	12.84	11.35	10.89
ANFIS	0.96	0.922	4.52	8.30	7.51

Table 2. Error measures for location of maximum scour from bucket

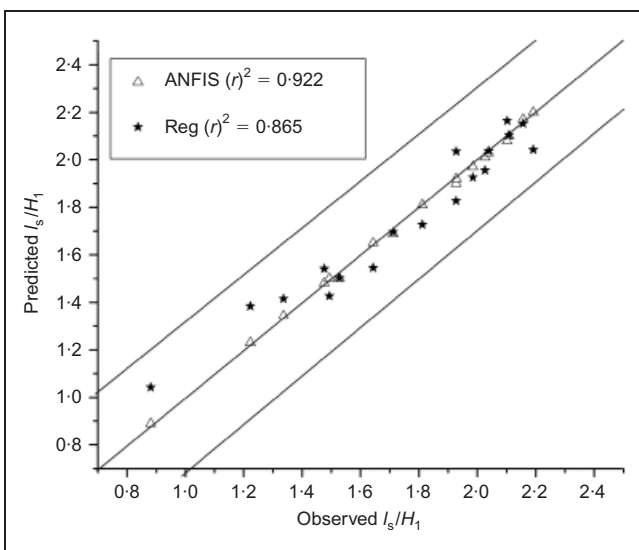


Figure 5. Comparison of measured and computed relative scour location

ANFIS gives a more accurate prediction compared with regression Equation 16. The software code is available by an email request to the first author of the current paper (redacazamath@eng.usm.my, mdazmath@gmail.com).

7. CONCLUSIONS

The data on hydraulic model studies, in respect of scour depth and the distance of maximum scour from bucket lip due to an outflow of horizontal jet issuing from trajectory bucket spillway, were analysed. A fit of statistical non-linear regression to these data yielded Equation 16, which is recommended in order to predict the location of maximum scour depth for the preliminary design for the scour location. Using the recommended ANFIS network, the computed scour location has a much closer agreement with the actual measured values.

It is possible to obtain a prediction of the location of scour with greater accuracy. The use of the parameters of R , d_{50} , d_w and ϕ would be necessary in addition to those of q and H_1 as

practised in traditional formulae, if more accurate predictions are desired.

Further research on spillway scour based on the prototype data such as the type of rock bed, classified as per rock quality designation, and rock mass rating by using genetic programming is under way.

8. APPENDIX I. THE ANFIS NETWORK

This network (Figure 3) works as follows. Let x and y be the two typical input values fed at the two input nodes, which will then transform those values to the membership functions (say bell-shaped) and give the output as follows (note in general, w is the output from a node; μ is the membership function, A_i ; and B_i is the fuzzy sets associated with nodes x, y).

$$19 \quad \mu_{A_i}(x) = \frac{1}{1 + |(x - c_1)/a_1|^{2b_1}}$$

where a_1, b_1 and c_1 are the changeable premise parameters. Similar computations are carried out for the input of y to obtain $\mu_{B_i}(y)$. The membership functions are then multiplied in the second layer, for example

$$20 \quad w_i = \mu_{A_i}(x)\mu_{B_i}(y) \quad (i = 1, 2)$$

Such products or firing strengths are then averaged

$$21 \quad \bar{w}_i = w_i / \sum w_i \quad (i = 1, 2)$$

Nodes of the fourth layer use the above ratio as a weighting factor. Furthermore, using fuzzy IF-THEN rules produces the following output (an example of an IF-THEN rule is: if x is A_1 and y is B_1 , then $f_1 = p_1x + q_1y + r_1$)

$$22 \quad \bar{w}_i f_i = \bar{w}_i (p_i x + q_i y + r_i)$$

where p, q and r are the changeable consequent parameters. The final network output f is produced by the node of the fifth layer as summation of all incoming signals, which is exemplified in Equation 22.

A two-step process is used for faster training and to adjust the network parameters to the above network. In the first step, the premise parameters are kept fixed, and the information is propagated forward in the network to layer 4. In layer 4, a least-squares estimator identifies the important parameters. In the second step, the backward pass, the chosen parameters are held fixed while the error is propagated. The premise parameters are then modified using gradient descent. Apart from the training patterns, the only user-specified information required is the number of membership functions for each input. The description of the learning algorithm is given in Jang and Sun.³⁴

9. APPENDIX 2. THE ERROR MEASURES

Correlation coefficient (r)

$$23 \quad r = \frac{\sum xy}{\sqrt{\sum x^2 \sum y^2}}$$

where $x = (X - \bar{X})$, $y = (Y - \bar{Y})$, X is observed values, \bar{X} is the mean of X , Y is the predicted value, \bar{Y} is the mean of Y . The summation in the above equation as well as in the following two equations is carried out over all n number of testing patterns.

Coefficient of determination (r^2)

$$24 \quad r^2 = \left(\frac{\sum xy}{\sqrt{\sum x^2 \sum y^2}} \right)^2$$

Average error (AE)

$$25 \quad AE = \frac{\sum [(X - Y)/X] 100}{n}$$

Mean square error (MSE)

$$26 \quad MSE = \frac{\sum (X - Y)^2}{n}$$

Average absolute deviation, d

$$27 \quad d = \frac{\sum |(Y - X)|}{\sum X} \times 100$$

ACKNOWLEDGEMENTS

The authors wish to express their sincere gratitude to Universiti Sains Malaysia for funding a short-term grant (304.PREDAC.6035262) to conduct this ongoing research. The authors are grateful to Dr M. C. Deo, Professor and Head of Civil Engineering, IIT Bombay, for his invaluable guidance and providing recent literature. The authors also thank Chang Chun Kiat and Leow Cheng Siang, REDAC officers, for their invaluable help in the preparation of this manuscript.

REFERENCES

1. AZAMATHULLA H. M., DEO M. C. and DEOLALIKAR P. B. Alternative neural networks to estimate the scour below spillways. *Advances in Engineering Software*, 2008, 39, No. 8, 689–698.
2. JANG J. S. R. ANFIS: Adaptive network based fuzzy inference system. *IEEE Transactions Systems, Man and Cybernetics*, 1993, 23, No. 3, 665–685.
3. JANG J. S. R. and GULLEY N. *Fuzzy Logic Toolbox User's Guide*. The Mathworks, Inc., Natick, MA, 1995.
4. KELLER J. M., YAGER R. R. and TAHANI H. Neural network implementation of fuzzy logic rules with neural networks. *International Journal of Approximate Reasoning*, 1992, 6, No. 2, 221–240.
5. KELLER J. M., KRISHNAPURAM R. and RHEE F. C. H. Evidence

- aggregation networks for fuzzy logic interface. *IEEE Transactions Neural Networks*, 1992, 3, No. 5, 761–769.
6. TAKAGI H. and HAYASHI I. NN-driven fuzzy reasoning. *International Journal Approximate Reasoning*, 1991, 5, No. 3, 191–212.
 7. HORIKAWA S., FURUHASHI T. and UCHIKAWA Y. On fuzzy modeling using fuzzy neural networks with the back-propagation algorithm. *IEEE Transactions Neural Networks*, 1992, 3, No. 5, 801–806.
 8. KOSKO B. *Neural Networks and Fuzzy Systems*. Prentice Hall, Englewood Cliffs, NJ, 1992.
 9. MAITRE R. and BOLENSKY S. Etuded quelques caractéristiques de l'écoulement dans la partie aval des évacuateurs de surface. *La Houille Blanche*, Grenoble, France, 1954, 481–511.
 10. HORENI P. The free decay study of the beam in air Workbook 93, Work and Study, Hydraulic Research Institute, Prague, Czechoslovakia. 1956. In Czech.
 11. ELEVATORSKI E. A. Trajectory bucket-type energy dissipators. *Proceedings of ASCE, Journal of the Power Division*, 1958, 84, No. 2, Paper No. 1553, 1–15.
 12. KAWAKAMI. K. A study of the computation of horizontal distance of jet issued from ski-jump spillway. *Japanese Society of Civil Engineering Journal*, 1973, 219, No. 11, 37–44.
 13. ELSAWY E. M and MCKEOGH E. J. Study of self aerated flow with regard to modelling criteria. *Proceedings of the 17th Congress of the IAHR*, 1977, A60, 475–482.
 14. TARAIMOVICH I. I. Deformation of channels below high head spillways on rock foundations. *Hydro Technical Construction (USSR)*, 1978, 8, No. 9, 917–923.
 15. KOBUS H., LEISTER P. and WESTRICH B. Flow field scouring effect of steady and pulsating jets impinging on a movable bed. *Journal of Hydraulic Research*, 1979, 1–7, No. 3, 175–192.
 16. SEN P. Spillway scour and design of plunge pool. *Journal of Irrigation and Power, CBIP, India*, 1984, 41, No. 1, 51–66.
 17. LOCHER F. A. and HSU S. T. Energy dissipation at high dams. In *Development in Hydraulic Engineering* (NOVAK P. (ed.)). Elsevier, London, 1984, Vol. 2, pp. 183–238.
 18. BORMANN N. E. and JULIEN P. Y. Scour downstream of grade-control structures. *Journal of Hydraulic Engineering, ASCE*, 1991, 117, No. 5, 579–594.
 19. BREUSERS H. N. C. and RAUDKIVI A. J. *Scouring*. IAHR, Rotterdam/Brookfield, 1991.
 20. ZHENGHU. D. Model tests and prototype observations for throw distances of jets and erosion of downstream riverbed at Wujiangdu hydropower station. *Proceedings of a National Symposium on Hydraulic Research in Nature and Laboratory*, Wuhan, 1992, pp. 365–371.
 21. AMANIAN N and GILBERTO E. U. Design of pre-excavated scour hole below flip bucket spillways. *Proceedings of the 1993 ASCE National Conference on Hydraulic Engineering*, San Francisco, 1993, pp. 856–860.
 22. TAO H. Scale effects of overflow-oriented hydraulic parameters for a high dam. *Proceedings of the ASCE Hydraulic Engineering Conference*, San Diego, CA, 1990, pp. 366–371.
 23. MASON P. J. Effect of air entrainment on plunge pool scour. *Journal of Hydraulic Engineering, ASCE*, 1993, 115, No. 3, 385–399.
 24. RAE P. J. and DIANA H. C. Estimation of spillway jet trajectory lengths. *Proceedings of the ASCE National Conference on Hydraulic Engineering*, Buffalo, NY, 1994, pp. 421–425.
 25. HOFFMANS G. J. C. M. and VERHEIJ H. J. *Scour Manual*. A. A. Balkema, Rotterdam/Brookfield, 1997.
 26. HOFFMANS G. J. C. M. Jet scour in equilibrium phase. *ASCE Journal of Hydraulic Engineering*, 1998, 124, No. 4, 430–437.
 27. GHODSIAN M., ARDESHIR A. F. and ALI A. A. Scour downstream of free over fall spillway. *Proceedings of the 28th IAHR Conference*, Graz, Austria, 1999.
 28. ROMAN J. and HAGER W. H. Trajectory bucket without and with deflectors. *Journal of Hydraulic Engineering, ASCE*, 2000, 126, No. 11, 837–845.
 29. STEFANO C. and HAGER W. H. Effect of air content on plunge pool scour. *Journal of Hydraulic Engineering, ASCE*, 2003, 129, No. 5, 358–365.
 30. PANASENKOV N. S. Effect of the turbulence of a liquid jet on breakdown. *Zurnal Techniceskoj fiziki*, 1951, 21, 161–166.
 31. BUREAU OF INDIAN STANDARDS. *Criteria for hydraulic design of bucket type energy dissipators*. BIS, 1985, BIS: New Delhi, India, 7365, 2nd revision.
 32. WASSERMAN P. D. *Advanced Methods in Neural Computing*. Van Nostrand Reinhold, New York, 1993.
 33. LONDHE S. N. and DEO M. C. Wave tranquility studies using neural networks. *Marine Structures*, 2003, 16, No. 6, 419–436.
 34. JANG J. S. R. and SUN C. T. Neuro-fuzzy modelling and control. *Proceedings of IEEE*, 1995, 83, No. 3, 378–406.
 35. TAY J. H. and ZHANG X. Neural fuzzy modeling of anaerobic biological waste water treatment systems. *Journal of Environmental Engineering, ASCE*, 1999, 125, No. 12, 1149–1159.
 36. NAYAK P. C., SUDHEER K. P., RANGAN D. M. and RAMASASTRI K. S. A neuro-fuzzy computing technique for modelling hydrological time series. *Journal of Hydrology*, 2004, 291, No. 12, 52–66.
 37. SAYED T., TAVAKOLIE A. and RAZAVI A. Comparison of adaptive network based fuzzy inference systems and B-spline neuro-fuzzy mode choice models. *Journal of Computers in Civil Engineering*, 2003, 17, No. 2, 123–130.
 38. AKBULBUT S., SAMET HSILOGLU A. and PAMUKEN S. Data generation for shear modulus and damping ratios in reinforced sands using adaptive neuro fuzzy inference system. *Soil Dynamics and Earthquake Engineering*, 2004, 24, No. 11, 805–814.

What do you think?

To discuss this paper, please email up to 500 words to the editor at journals@ice.org.uk. Your contribution will be forwarded to the author(s) for a reply and, if considered appropriate by the editorial panel, will be published as discussion in a future issue of the journal.

Proceedings journals rely entirely on contributions sent in by civil engineering professionals, academics and students. Papers should be 2000–5000 words long (briefing papers should be 1000–2000 words long), with adequate illustrations and references. You can submit your paper online via www.icevirtuallibrary.com/content/journals, where you will also find detailed author guidelines.